SorCS1 binds the insulin receptor to enhance insulin sensitivity.

Mads Kjolby[1,2,3*#], Karen Marie Pedersen[1,3*], Peter Breining[1,3*], Niels Wellner[1,3], Karen Marie Juul Sørensen[1,3,4], Dorthe Maria Vittrup[3], Anette Marianne Prior Gjesing[5], Dovile Januliene[4], Arulmani Manavalan[6], Maarten Rotman[6], Gangadaar Thotakura[6], Sune Skeldal[3], Peder Madsen[3], Søren Thirup[4], Guido Hermey[7], Christian B. Vaegter[3], Arne Möller[4,8], Olof Asplund[9], Rashmi B. Prasad[9], Edwin T. Parlevliet[10], Patrick C.N. Rensen[10], Ernst Martin Füchtbauer[11], Andreas Nygaard Madsen[12], Birgitte Holst[12], Olav M. Andersen[1,3], Torben Hansen[5] , and Anders Nykjaer[1,3,6, 13,#].

[1]PROMEMO and DANDRITE, Aarhus University, Denmark; [2]Department of Clinical Pharmacology, Aarhus University Hospital, Denmark and Danish Diabetes Academy; [3]Department of Biomedicine, Aarhus University, Denmark; [4]Department of Molecular Biology, Aarhus University; [5]Novo Nordisk Foundation Center for Basic Metabolic Research, Copenhagen University, Denmark; [6]Department of Neuroscience, Mayo Clinic, Florida, USA; [7]Institute for Molecular and Cellular Cognition, Center for Molecular Neurobiology Hamburg, University Medical Center Hamburg-Eppendorf; [8]Osnabrück University, Frankfurt Am Main Area, Germany; [9]Lund University Diabetes Centre, Malmö, Sweden; [10]Dept. Medicine, Div. Endocrinology, and Einthoven Laboratory for Experimental Vascular Medicine, Leiden University Medical Center (LUMC), Leiden, The Netherlands; [11]Department of Molecular Biology and Genetics, Aarhus University, Denmark; [12]RMPC, Department of Biomedical Sciences, Copenhagen University, Denmark; [13]Department of Neurosurgery, Aarhus University Hospital, Denmark. * Shared first authors. #Corresponding authors

Anders Nykjaer
PROMEMO and DANDRITE
Department of Biomedicine
Hoegh-Guldbergsgade 10,
Aarhus University
DK-8000 Aarhus C
Denmark
Phone: +45 2899 2384
Email:an@biomed.au.dk

Mads Kjolby
DANDRITE
Department of Biomedicine,
Hoegh-Guldbergsgade 10,
Aarhus University
DK-8000 Aarhus C
Denmark
Phone: +45 6086 6653
Kjolby@biomed.au.dk

Word count: 2579 words, excluding title, authors, figure legends and references.

Type II diabetes mellitus (T2DM) has reached endemic levels and comprises a substantial burden to the patient and the society. Along with lifestyle factors, a number of genetic loci predisposing to T2DM have been suggested including *SORCS1* that encodes a type-1 transmembrane receptor. Here we establish SorCS1 as a high-affinity binding partner for the insulin receptor (IR) that increases insulin affinity, Akt activation, and peripheral glucose uptake. Mice lacking full-length SorCS1 develop age-dependent insulin resistance characterized by increased plasma glucose and insulin levels and a blunted response to exogenous insulin. SorCS1 exists in three forms; as a transmembrane monomer and dimer, and as a truncated soluble form (sol-SorCS1) produced in adipose tissue and is present in plasma. Whereas dimeric SorCS1 engages the proform of the insulin receptor (proIR) during biosynthesis and supports its maturation, the monomeric form stabilizes the mature IR at the plasma membrane. In its soluble form, SorCS1 positively correlates with body mass index and inversely with plasma glucose in diabetic patients, and in mouse models of insulin resistance, overexpression or exogenous administration of the monomeric soluble receptor domain restores insulin sensitivity. We conclude that SorCS1 is a critical regulator of peripheral insulin sensitivity operating in both a cell autonomous and endocrine manner, and we propose sol-SorCS1 as a novel adipokine.

17 The mechanisms controlling insulin sensitivity and glucose metabolism are fundamental to all
18 vertebrates. Skeletal muscle is essential to acutely buffer high plasma glucose and reduced insulin
19 sensitivity is affected very early on in the development of type 2 diabetes[1,2]. The downstream signaling
20 pathways of IR in skeletal muscle (e.g. Akt and mTOR) are well described, but whether insulin sensitivity
21 may be dynamically regulated at the level of the plasma membrane through interaction with co-receptors
22 or other membrane proteins is unknown[3-5]. The existence of such a molecular thermostat to adapt insulin
23 sensitivity to the metabolic state would transform our conceptual understanding on how key metabolic
24 processes can be controlled.

25 SorCS1 is a member of the Vps10p-domain family of sorting receptors that also comprises
26 sortilin, SorLA, SorCS2, and SorCS3[6,7]. Several studies have identified *SORCS1* as a risk locus for type
27 2 diabetes mellitus that is conserved in women[8-10], and in female rats[11] and mice[12]. Recently, SorCS1
28 was shown to facilitate the biogenesis of insulin containing secretory granules, but a function outside the
29 β-cells was not studied[13]. The structurally related receptor sortilin can function in the secretory pathway
30 by assisting hepatic lipoprotein export[14-16], while in neurons it physically interacts with tropomyosin
31 receptor kinases (Trks) to enable their surface exposure and signaling capacity[17]. We hypothesized that
32 SorCS1 likewise may engage a tyrosine kinase receptor to promote its activity. Given the genetic
33 association with T2DM we here asked whether this tyrosine kinase receptor could be IR.

34 SorCS1 exists in several isoforms comprising an identical extracellular domain encoded by
35 exons 1-24 but with at least four distinct sorting competent cytoplasmic tails (a, b, c, and d)[18,19] resulting
36 from alternative splicing from exons 25 to 28 (exon 25 also encodes the transmembrane domain)
37 (**Extended Data Fig. 1**). Regardless the isoform, the extracellular domain (sol-SorCS1) can be efficiently
38 liberated from the plasma membrane by ADAM17/TACE mediated cleavage[20] but the biological

39 relevance of this is unknown. To investigate the function specifically of the full-length receptor variants
40 we generated a mouse model (*Sorcs1*$^{\Delta 25\text{-}28}$), in which exons 25-28 had been deleted leaving the first 24
41 exons intact to allow production of only sol-SorCS1 (**Extended Data Fig. 1**). RT-PCR for *Sorcs1* in
42 brain, adipose tissue and muscle extracts confirmed that exons 25-28 had been deleted whereas the
43 extracellular domain encoded by exons 1-24 were transcribed.

44 Starting from 23 weeks of age, female *Sorcs1*$^{\Delta 25\text{-}28}$ mice fed a normal chow developed
45 hyperglycemia. This was paralleled by elevated plasma insulin levels (**Fig. 1a-b**). The hyperinsulinemia
46 progressively increased as animals aged, reaching 4.6-fold higher insulin levels in 50 weeks old
47 compared 10 weeks old mice, and twice the concentration in wildtype controls at 50 weeks. Consistent
48 with genetic studies in mice, rats and humans[8-12], the glycemic phenotype was present only in female
49 *Sorcs1*$^{\Delta 25\text{-}28}$ mice inasmuch plasma glucose in the male transgenics remained normal up till 60 weeks of
50 age (**Extended Data Fig. 2**). An oral glucose tolerance test (OGTT) confirmed that glucose handling
51 was impaired in the females. Hence, in 14 months old *Sorcs1*$^{\Delta 25\text{-}28}$ mice plasma glucose peaked at 15.7
52 mM compared to 12. 6 mM for their littermate controls and it returned slower to baseline, corresponding
53 to a 45% increase in the area under the curve (282 vs. 506 mM*min) (**Fig. 1 c-d**).

54 The perturbed glucose homeostasis was most pronounced when comparing littermates from
55 heterozygous breeding on a mixed C57BL/6BomTac x 129sv genetic background (**Fig. 1a-d**). However,
56 reduced peripheral insulin sensitivity was also evident in 47 weeks old C57BL/6BomTac congenic
57 female mutant mice when subjected to hyperinsulinemic euglycemic clamp[21,22] (**Fig. 1e-f and Extended**
58 **Figs. 3a-b**). At the beginning of the experiment, plasma glucose did not differ between genotypes and
59 neither did peripheral glucose uptake nor hepatic glucose production. However, when continuously
60 infusing a similar concentration of insulin (**Extended Data Fig. 3c**) we observed a 37% weaker glucose-

61 suppressing effect at euglycemic levels in the *Sorcs1*$^{\Delta 25\text{-}28}$ mutants compared to wildtype mice (**Fig. 1e**).
62 This difference was solely accounted for by reduced peripheral glucose uptake since hepatic glucose
63 production had been fully shutdown (**Fig. 1f and Extended Fig. 3b**).

64 To assess peripheral glucose uptake, we examined the role of SorCS1 on IR signaling in
65 muscle extracts, in primary differentiated myocytes, and in the myocyte-derived cell line C2C12. In 19
66 weeks old normoglycemic female mice administration of an insulin bolus potently stimulated IR
67 phosphorylation (pIRβ) in skeletal muscle of both *Sorcs1*$^{\Delta 25\text{-}28}$ mutant animals and their littermate
68 controls. In marked contrast, at 50 weeks of age, when *Sorcs1*$^{\Delta 25\text{-}28}$ mice were diabetic, pIR was now
69 substantially compromised (**Fig. 2a**). A blunted insulin response was also present in primary *Sorcs1*$^{\Delta 25\text{-}}$
70 ^{28} myocyte cultures, as more than 10-fold higher insulin concentrations were required to activate IR in
71 the mutant cultures compared to those from wildtype mice (**Fig. 2b**). Finally, we studied insulin
72 stimulated AKT signaling in C2C12 cells after CRISPR/Cas9 knockout of *Sorcs1*. Corroborating the data
73 in the primary myocytes, C2C12 knockout cells were less insulin responsive as the EC50 curve for pAKT
74 was right-shifted approximately five-fold (**Fig. 2c**). In the mutant *Sorcs1*$^{\Delta 25\text{-}28}$ myocyte cultures we
75 observed a band with a molecular weight smaller than that of the IR_{β}-chain (**Fig. 2b**). Surface
76 biotinylation experiments revealed that this band was restricted to the interior of the cells indicating a
77 degradation product of proIR or IR. Possibly as a consequence, IR_{β} expression at the plasma membrane
78 was reduced by up to 60% in the *Sorcs1*$^{\Delta 25\text{-}28}$ cultures (**Fig. 2d**). Impaired N-glycosylation of proIR
79 prevents two-chain processing and leads to degradation of the pro-receptor[23]. In the mutant myocytes we
80 observed in addition to mature proIR a species of lower molecular weight (**Fig. 2e**). Treatment with
81 PNGase F to remove N-linked oligosaccharides identified this protein as immature non-glycosylated

82 proIR. Taken together the data argue that intracellular SorCS1 facilitates glycosylation and maturation
83 of proIR and prevents its degradation.

84 We next asked whether surface exposed SorCS1 may also control IR activity. To this end,
85 IR was overexpressed in HEK 293 cells alone or in combination with SorCS1-b, an isoform that is
86 enriched at the plasma membrane and incapable of endocytosis and sorting[24]. Co-expression with SorCS1
87 increased insulin affinity to IR by approximately five-fold (**Fig. 3a**). To assess whether a physical
88 interaction between SorCS1 and IR could be involved we employed surface plasmon resonance (SPR)
89 analysis using the extracellular domains of SorCS1 (sol-SorCS1) and IR. The SPR analysis showed that
90 sol-SorCS1 binds to immobilized IR with an estimated affinity of 5 nM (**Fig. 3b**). Importantly, binding
91 of insulin to IR did not inhibit its interaction with SorCS1, indicating formation of a trimeric complex
92 (**Fig. 3c**). No binding was observed for insulin, pro-insulin, glucagon, or glucagon-like peptide 1 (GLP-
93 1) to SorCS1 (**Extended Data Fig. 4a**). To demonstrate that SorCS1, IR, and insulin can physically
94 interact at the plasma membrane we performed immunoprecipitation (IP) experiments in HEK293 cells
95 co-transfected with SorCS1 and IR in the absence or presence of insulin (**Fig. 3d**). Antibodies against IR
96 co-precipitated SorCS1 and vice versa and this interaction was unaffected by preincubation with 100 nM
97 insulin. Notably, IP of SorCS1 also co-precipitated proIR, which supports its role in facilitating N-linked
98 glycosylation of the receptor in the biosynthetic pathway.

99 SorCS1 exists as a non-covalent dimer and in a monomeric form, the conformational state
100 of which is regulated by the level of glycosylation[25]. While unglycosylated receptor is a dimer,
101 maturation with N-linked oligosaccharides converts it into a monomer[25]. We asked whether the
102 stoichiometric state may regulate the preference of SorCS1 for proIR or IR. To elucidate this, HEK293
103 cells expressing endogenous IR were co-transfected with two SorCS1 constructs where the cytoplasmic
104 tail had been substituted by a FLAG- and Myc-tag, respectively. The cells were then subjected to

105 sequential co-immunoprecipitation, first with anti-FLAG and after elution from the beads subsequently
106 with anti-Myc (**Fig. 3e, Extended Data Fig. 4b**). Immunoprecipitation with anti-FLAG-coated beads
107 precipitates receptor populations that comprise a mixture of monomers (SorCS1-FLAG) and dimers
108 (SorCS1-FLAG/FLAG and SorCS1-FLAG/Myc). After elution from the beads followed by the second
109 round of IP using anti-Myc antibodies only dimeric SorCS1 will be left (SorCS1-FLAG/Myc) (**Fig. 3e**).
110 Anti-FLAG immunoprecipitated in addition to the Myc-tagged SorCS1 both proIR and mature IR.
111 However, following the successive co-IP with anti-Myc to select for dimeric SorCS1, only proIR was
112 now co-immunoprecipitated. We conclude that dimeric SorCS1 is specific for proIR whereas monomeric
113 SorCS1 can bind mature IR. To explore the spatial distribution of these interactions, we used a
114 bimolecular fluorescence complementation (BiFC) assay[26]. HEK293-IR cells were transfected with two
115 human SorCS1 constructs each containing one-half of the Venus fluorescent protein. When SorCS1
116 dimerizes the two Venus fragments unite to elicit a green fluorescent signal that echoes the subcellular
117 distribution of dimeric SorCS1. First, we stained the cells with an antibody that recognizes both
118 monomeric and dimeric SorCS1 and found that only monomeric SorCS1 is present at the plasma
119 membrane as the BiFC-positive signal was restricted to intracellular compartments (**Fig. 3f**). We next
120 combined the BiFC signal with proximity ligation assay (PLA) for SorCS1 and IR. In this assay a red
121 fluorescent signal will appear when the receptors are in close proximity (<30 nm). In unpermeabilized
122 cells we observed a strong PLA signal at the plasma membrane that was BiFC-negative, indicating
123 binding of monomeric SorCS1 to mature IR (**Fig. 3g)**. In contrast, in permeabilized cells a strong PLA
124 signal was present in BiFC-positive intracellular structures compatible with the Golgi-compartment and
125 the endoplasmatic reticulum that is dispersed throughout the cytosol (**Fig. 3h**). Because these
126 compartments are enriched in proIR, the combined data suggest that monomeric SorCS1 engages IR at

127 the plasma membrane whereas the dimeric and not fully glycosylated receptor binds proIR in the
128 secretory pathway[25].

129 Both humans and mice express SorCS1 in skeletal muscle and adipose tissue (**Figs. 4a and**
130 **Extended Data Fig. 1c**). We previously reported that up to 95% of SorCS1 is shed per hour from the
131 plasma membrane by ADAM17/TACE mediated cleavage[20,24]. Given SorCS1 and IR can bind each other
132 through an interaction in their extracellular domains (cf. **Fig. 3b and c**), we hypothesized that soluble
133 SorCS1 could have a glycemic regulatory function. To address this, we studied IR signaling in
134 differentiated myocyte cultures from *Sorcs1*$^{\Delta 25\text{-}28}$ mice after insulin stimulation in the presence of
135 increasing concentrations of exogenous sol-SorCS1 (**Fig. 4b)**. Sol-SorCS1 augmented insulin induced
136 phosphorylation of IR and Akt and did so in a concentration dependent manner. No effect was observed
137 in the absence of insulin demonstrating that sol-SorCS1 is not an insulin mimetic. To establish a function
138 of sol-SorCS1 *in vivo*, we first compared the plasma concentration in a cohort of T2DM patients with
139 normoglycemic healthy individuals. In the diabetic group, but not among healthy individuals, plasma
140 glucose inversely correlated with sol-SorCS1 (**Fig. 4c**). Since differentiated 3T3-L1 adipocytes potently
141 liberates sol-SorCS1 (**Fig. 4d**) and human and murine adipose tissue express SorCS1 (**Fig. 4a, Extended**
142 **data Fig. 5)** alongside ADAM17/TACE[20], we examined, whether body mass index (BMI) associates
143 with the plasma concentration of sol-SorCS1. We found that BMI positively correlates with measures of
144 sol-SorCS1 both in diabetic individuals and healthy controls (**Extended Data Fig. 6**). The data suggested
145 that sol-SorCS1 may act as an adipokine to counteract the increased plasma glucose levels that commonly
146 follows obesity.

147 To establish a glucose lowering and insulin sensitizing effect of sol-SorCS1 *in vivo*, we
148 injected an adenovirus encoding human sol-SorCS1 (AV-sol-SorCS1) or AV-LacZ (encoding β-

149 galactosidase) as a negative control into the tail vein of obese leptin receptor knockout mice (*db/db*) that
150 develop severe T2DM. One week later, plasma glucose was increased by 55% and insulin by 65% in the
151 LacZ group due to the gradual worsening of the diabetic phenotype (**Fig. 4e-f**). Remarkably, in the AV-
152 sol-SorCS1 treated mice, plasma glucose remained unchanged and this despite a decrease in plasma
153 insulin. In an intraperitoneal glucose tolerance test (IPGTT), AV-sol-SorCS1 mice responded markedly
154 stronger with lower plasma glucose levels at all timepoints corresponding to a reduction in the area under
155 the curve (AUC) by 79.5% (**Fig. 4g-h)**. The treated animals also exhibited superior ability in mobilizing
156 insulin compared to the control group (**Fig. 4i).** A similar glucose and insulin reducing effect was
157 obtained in adenovirus treated male mice with dietary induced T2DM (**Extended Data Fig. 7**). Next we
158 performed hyperinsulinemic euglycemic clamp[22]. AV-sol-SorCS1 mice showed lower basal plasma
159 glucose and increased capacity for glucose uptake compared to AV-LacZ treated animals (**Fig. 4j and**
160 **k**). Glucose tracer studies revealed that this effect was accounted for by increased insulin sensitivity in
161 peripheral tissues (**Fig. 4l, Extended Fig. 8**). Notably, three weeks post injection, glycated hemoglobin
162 (HbA1c) had increased considerably in the AV-LacZ group but it stayed unchanged in the AV-sol-
163 SorCS1 group indicating a long-lasting beneficial effect of the soluble receptor in reducing plasma
164 glucose (**Fig. 4m**).

165 In cells, full-length dimeric SorCS1 binds exclusively to the proIRs whereas monomeric
166 SorCS1 recognizes mature IR (**Fig 3e-h**). Hence, we speculated that the active form of sol-SorCS1
167 liberated by ADAM17 mediated cleavage is the monomer. To demonstrate this, we purified monomeric
168 and dimeric sol-SorCS1 from transfected CHO cells and injected *db/db* mice with each form
169 intraperitoneally 10 hrs and 1 hr prior to glucose tolerance test. Intriguingly, monomeric sol-SorCS1, but
170 not the dimeric receptor, profoundly improved glucose tolerance (**Fig. 4n**). Hence, the AUC for plasma

171 glucose was reduced by approximately 60% (from 1060 to 393 mM*min, $P<0.05$) in animals treated with
172 monomeric sol-SorCS1 (**Fig. 4o**).

173 In conclusion, we have demonstrated that full-length SorCS1, expressed in peripheral
174 tissues augments insulin sensitivity by engaging proIR and IR; the dimeric SorCS1 binds intracellular
175 proIR and the monomeric receptor the surface exposed mature IR. As a soluble protein, monomeric
176 SorCS1 can target tissues remote from where it is being produced (**Extended Data Fig. 9**). Given SorCS1
177 is expressed in adipose tissue, that it can be shed from adipocytes, and that its plasma concentration
178 positively correlates with BMI, we propose sol-SorCS1 as a novel adipokine to enhance insulin
179 sensitivity.

180

181 **Acknowledgements**

182 The study was funded by the Lundbeck Foundation grant no. R248-2017-431 (AN) , DANDRITE-R248-
183 2016-2518 (AN), R90-2011-7723 (AN); The Independent Research Fund Denmark grant no. DFF-7016-
184 00261 (AN); The Novo Nordisk Foundation grant no. NNF16OC0020984 (AN); The Danish National
185 Research Foundation grant no. DNRF133 (AN); The Danish Diabetes Academy (MK). We thank
186 Benedicte Vestergaard, Anja Aagaard and Anne Kerstine Thomassen for excellent technical assistance.

187

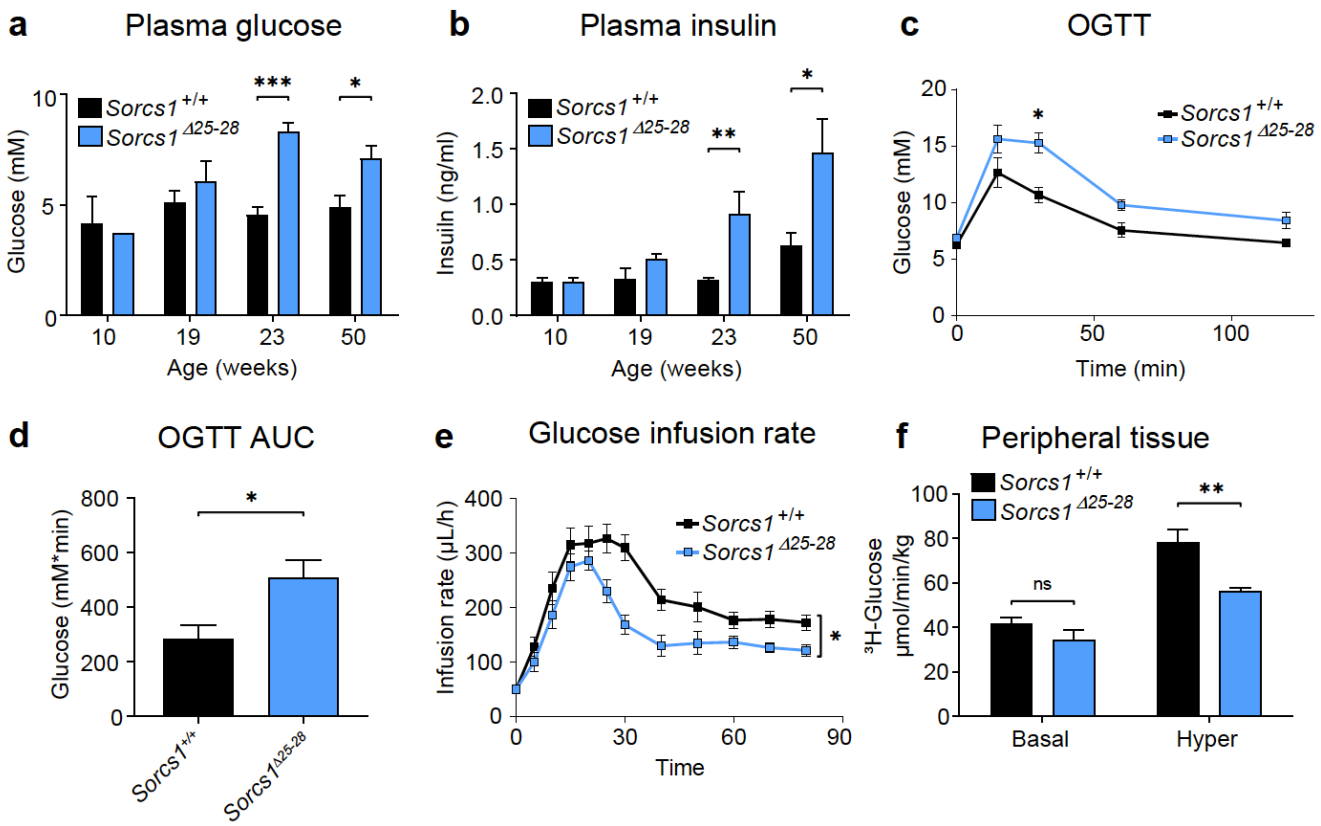

Figure 1: Insulin resistance and T2DM in *Sorcs1*$^{\Delta 25\text{-}28}$ mice.

a, Plasma glucose and, **b**, insulin concentrations in aging female *Sorcs1*$^{\Delta 25\text{-}28}$ mice (wildtype n=4, *Sorcs1*$^{\Delta 25\text{-}28}$ n=9). **c**, Impaired glucose tolerance in 50 weeks old female *Sorcs1*$^{\Delta 25\text{-}28}$ mice. **d**, AUC of the data in **c** calculated minus baselines at t=0 (wildtype n=7, *Sorcs1*$^{\Delta 25\text{-}28}$ n=10). **e**, In hyperinsulinemic euglycemic clamp, glucose infusion rate (GIR) is lower in *Sorcs1*$^{\Delta 25\text{-}28}$ female mice at steady state (t=60-90 min). **f**, The insulin resistance is peripheral (wildtype n=7, *Sorcs1*$^{\Delta 25\text{-}28}$ n=6). Data are presented as mean ± SEM, * = P<0.05, ** = P<0.01.

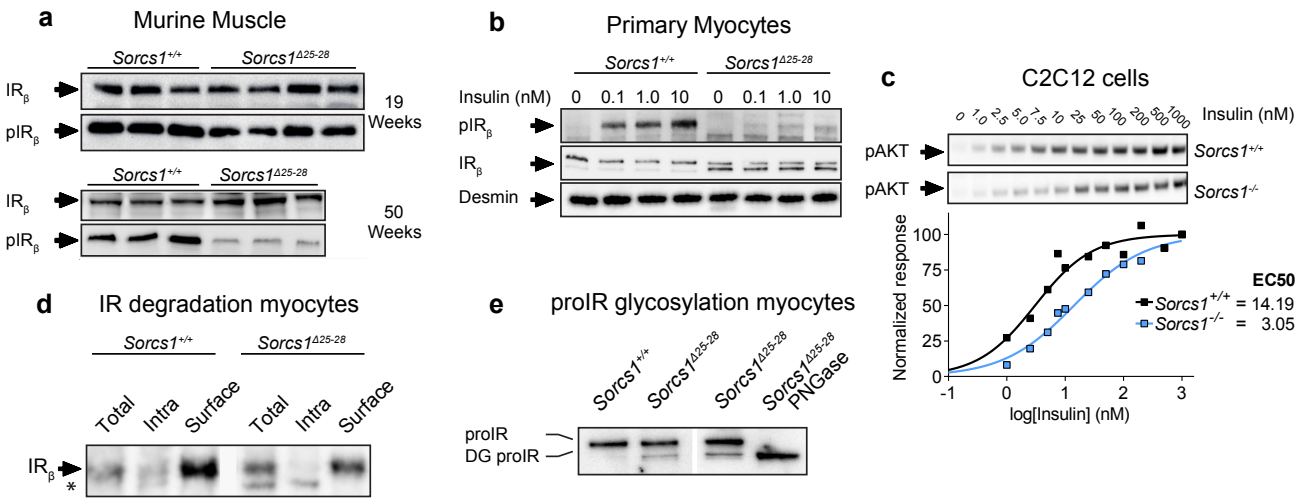

Figure 2: Impaired insulin receptor signaling in *Sorcs1*$^{\Delta 25\text{-}28}$ muscle.

a, IR phosphorylation is reduced in 50 but not in 19 weeks old female mutant mice, 15 min post insulin injection. **b**, Impaired insulin-induced IR phosphorylation in differentiated primary myocytes from *Sorcs1*$^{\Delta 25\text{-}28}$ mice. Expression of desmin confirms the cultures are equally differentiated. **c**, Reduced phosphorylation of AKT in *Sorcs1*$^{-/-}$ C2C12 cells. **d**, Surface biotinylation of *Sorcs1*$^{\Delta 25\text{-}28}$ primary myocytes shows reduced IRβ expression at the plasma membrane and accumulation of an intracellular IRβ immunoreactive fragment. Asterisk indicate the low molecular weight band. **e**, PNGase treatment reveals reduced N-linked glycosylation of proIR in *Sorcs1*$^{\Delta 25\text{-}28}$ myocyte cultures. DG proIR designates deglycosylated proIR.

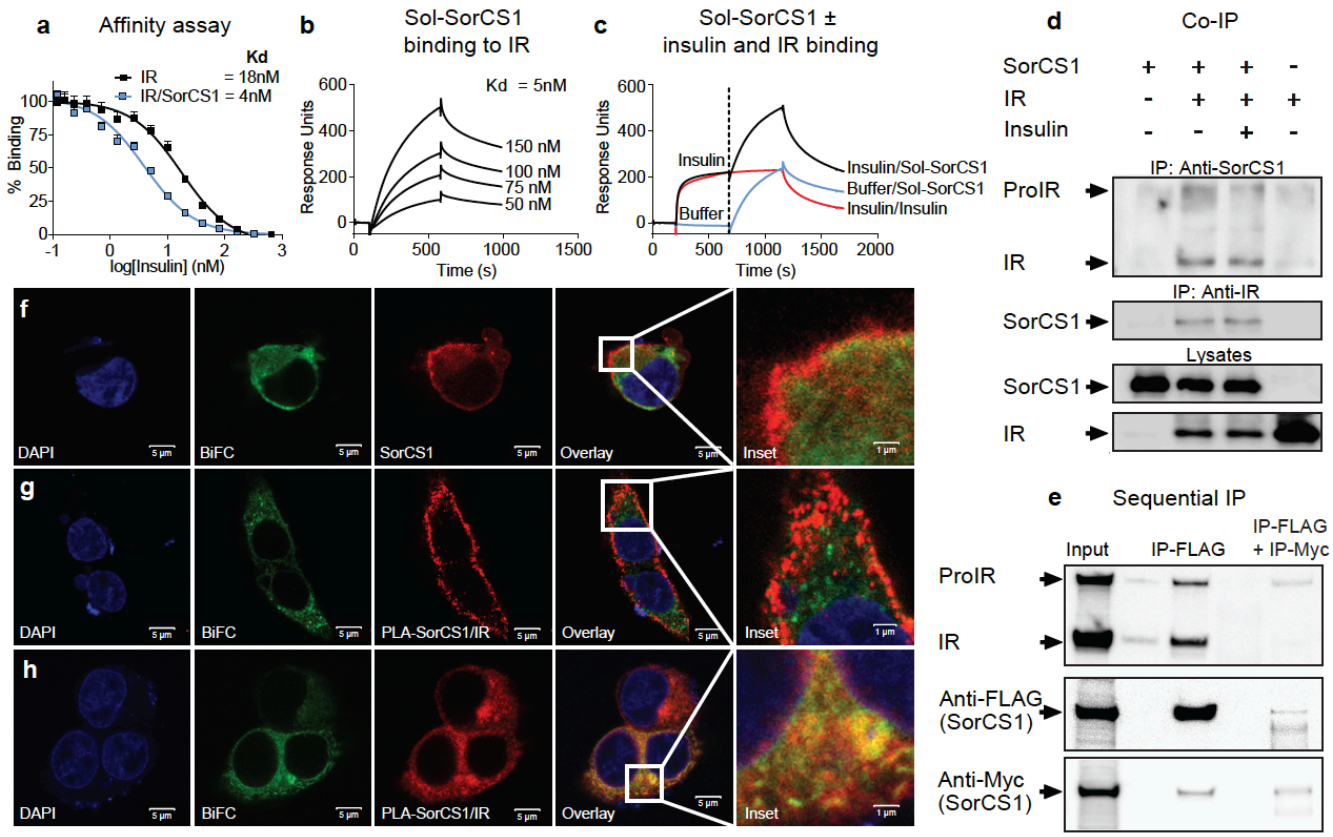

Figure 3: SorCS1 and IR physically interact.

a, SorCS1 overexpression in HEK293 cells increases insulin affinity to IR. **b**, SPR analysis demonstrates dose-dependent binding of sol-SorCS to IR. **c**, Complex formation of SorCS1, IR, and insulin determined by SPR. At 1200 sec, the additive signals for Sol-SorCS1 (*blue*) and insulin (*red*) equals the response units obtained when IR is incubated with both proteins simultaneously (*black*). **d**, Co-immunoprecipitation between SorCS1 and proIR/ IR. The interaction is independent on the presence of saturating concentrations of insulin (100 nM). **e**, Binding of dimeric SorCS1 is restricted to proIR, but monomeric SorCS1 can bind mature IR. **f**, SorCS1 dimers that are BiFC-positive (*green*) are confined to cytosolic compartments, whereas monomeric and BiFC-negative SorCS1 (*red*), is present at the cell surface (**f**, *inset*). **g**, In non-permeabilized HEK293, PLA for SorCS1 and IR (*red*) demonstrates binding

219 between monomeric SorCS1 (BiFC-negative) and IR. **h**, Dimeric SorCS1 (BiFC-positive, *green*)

220 interacts with pro-IR (*red*) in cytosolic compartment.

221

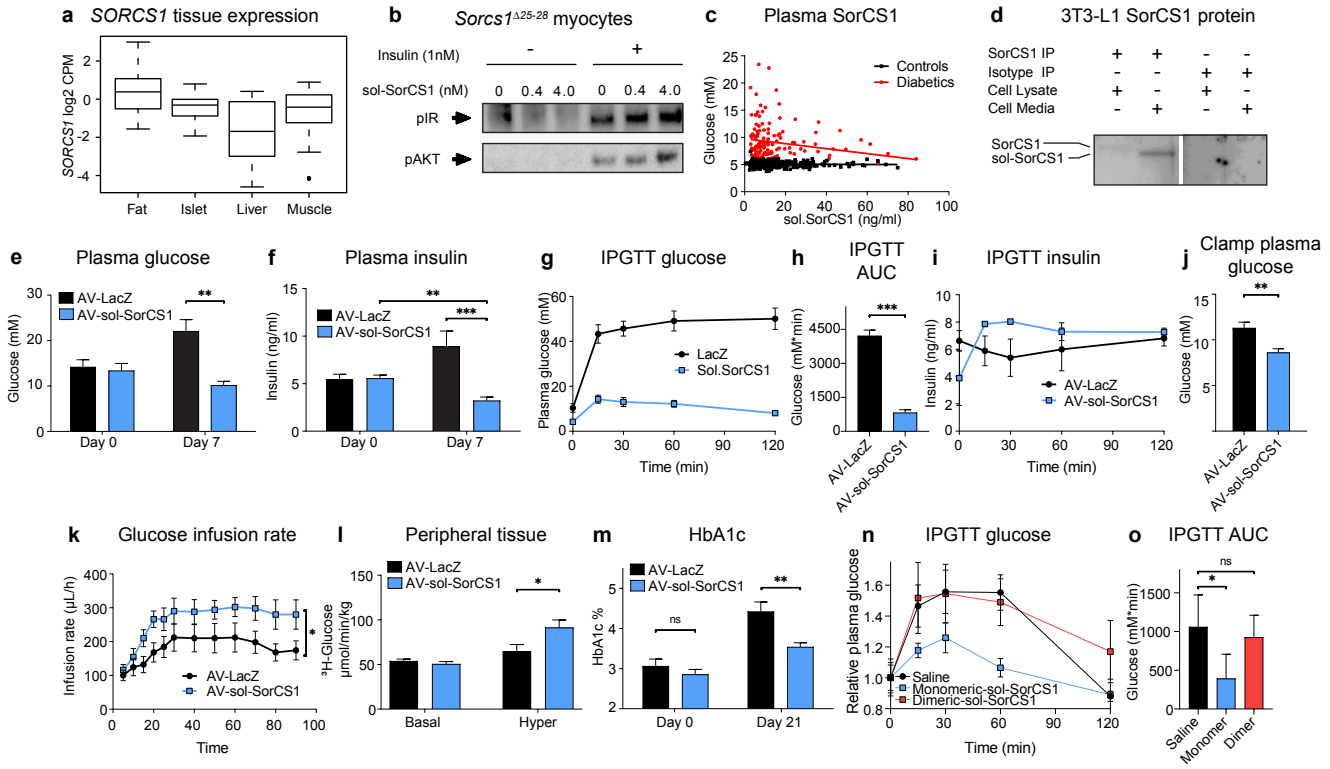

Figure 4: Sol-SorCS1 is an insulin sensitizer.

a, mRNA expression of SorCS1 in human tissues (n=12/group). **b**, Insulin-induced activation of IR and AKT in *Sorcs1*$^{\Delta 25\text{-}28}$ primary myocytes correlates with sol-SorCS1 concentration. **c**, In diabetic patients sol-SorCS1 in plasma negatively correlates with fasting plasma glucose (**β**-value -2.6E-3, P<0.001). **d**, Expression of full-length SorCS1 and shedding of its soluble form in 3T3-L1 adipocytes. **e**, Treatment with AV-sol-SorCS1, but not AV-LacZ, reduces plasma glucose levels and, **f**, plasma insulin in 7 weeks old *db/db* mice. **g**, Enhanced glucose uptake determined by IPGTT in AV-sol-SorCS1 treated *db/db* mice shown in real-time and, **h**, as AUC (n=4/group). **i**, Plasma insulin in the IPGTT shown in g-h. **j**, Lower fasting plasma glucose but, **k**, higher infusion rate in euglycemic hyperinsulinemic clamp of AV-sol-SorCS1 treated *db/db* mice (n=5/group). **l**, The higher infusion rate is accounted for by increased peripheral glucose uptake. **m**, Reduced HbA1c in *db/db* mice 21 days after infection with AV-sol-SorCS1

234 infection. **n**, Intraperitoneal injection of recombinant monomeric, but not dimeric, sol-SorCS1 increases

235 glucose tolerance (IPGTT) in *db/db* mice. **o**, AUC of the data displayed in panel **n**. Data are presented as

236 means ± SEM, * = $P<0.05$, ** = $P<0.01$, ***=$P<0.001$.

237 **References:**

238 1. Shanik, M.H., *et al.* Insulin resistance and hyperinsulinemia: is hyperinsulinemia the cart or the
239 horse? *Diabetes Care* **31 Suppl 2**, S262-268 (2008).

240 2. Warram, J.H., Martin, B.C., Krolewski, A.S., Soeldner, J.S. & Kahn, C.R. Slow glucose removal
241 rate and hyperinsulinemia precede the development of type II diabetes in the offspring of diabetic
242 parents. *Ann Intern Med* **113**, 909-915 (1990).

243 3. Kim, S.J., *et al.* mTOR complex 2 regulates proper turnover of insulin receptor substrate-1 via
244 the ubiquitin ligase subunit Fbw8. *Mol Cell* **48**, 875-887 (2012).

245 4. Tremblay, F., *et al.* Identification of IRS-1 Ser-1101 as a target of S6K1 in nutrient- and obesity-
246 induced insulin resistance. *Proc Natl Acad Sci U S A* **104**, 14056-14061 (2007).

247 5. Blagosklonny, M.V. TOR-centric view on insulin resistance and diabetic complications:
248 perspective for endocrinologists and gerontologists. *Cell Death Dis* **4**, e964 (2013).

249 6. Willnow, T.E., Petersen, C.M. & Nykjaer, A. VPS10P-domain receptors - regulators of neuronal
250 viability and function. *Nat Rev Neurosci* **9**, 899-909 (2008).

251 7. Willnow, T.E., Kjolby, M. & Nykjaer, A. Sortilins: new players in lipoprotein metabolism. *Curr*
252 *Opin Lipidol* **22**, 79-85 (2011).

253 8. He, Y., Fang, Z. & Yu, G. Sortilin-related VPS10 domain containing receptor 1 and Alzheimer's
254 disease-associated allelic variations preferentially exist in female or type 2 diabetes mellitus
255 patients in southern Han Chinese. *Psychogeriatrics* **12**, 215-225 (2012).

256 9. Paterson, A.D., *et al.* A genome-wide association study identifies a novel major locus for
257 glycemic control in type 1 diabetes, as measured by both A1C and glucose. *Diabetes* **59**, 539-549
258 (2010).

259 10. Goodarzi, M.O., *et al.* SORCS1: a novel human type 2 diabetes susceptibility gene suggested by
260 the mouse. *Diabetes* **56**, 1922-1929 (2007).
261 11. Granhall, C., Park, H.B., Fakhrai-Rad, H. & Luthman, H. High-resolution quantitative trait locus
262 analysis reveals multiple diabetes susceptibility loci mapped to intervals<800 kb in the species-
263 conserved Niddm1i of the GK rat. *Genetics* **174**, 1565-1572 (2006).
264 12. Clee, S.M., *et al.* Positional cloning of Sorcs1, a type 2 diabetes quantitative trait locus. *Nat Genet*
265 **38**, 688-693 (2006).
266 13. Kebede, M.A., *et al.* SORCS1 is necessary for normal insulin secretory granule biogenesis in
267 metabolically stressed beta cells. *J Clin Invest* **124**, 4240-4256 (2014).
268 14. Kjolby, M., *et al.* Sort1, encoded by the cardiovascular risk locus 1p13.3, is a regulator of hepatic
269 lipoprotein export. *Cell Metab* **12**, 213-223 (2010).
270 15. Kjolby, M., Nielsen, M.S. & Petersen, C.M. Sortilin, encoded by the cardiovascular risk gene
271 SORT1, and its suggested functions in cardiovascular disease. *Curr Atheroscler Rep* **17**, 496
272 (2015).
273 16. Mortensen, M.B., *et al.* Targeting sortilin in immune cells reduces proinflammatory cytokines
274 and atherosclerosis. *J Clin Invest* **124**, 5317-5322 (2014).
275 17. Vaegter, C.B., *et al.* Sortilin associates with Trk receptors to enhance anterograde transport and
276 neurotrophin signaling. *Nat Neurosci* **14**, 54-61 (2011).
277 18. Hermey, G., *et al.* SorCS1 variants and amyloid precursor protein (APP) are co-transported in
278 neurons but only SorCS1c modulates anterograde APP transport. *J Neurochem* **135**, 60-75 (2015).
279 19. Savas, J.N., *et al.* The Sorting Receptor SorCS1 Regulates Trafficking of Neurexin and AMPA
280 Receptors. *Neuron* **87**, 764-780 (2015).

281 20. Hermey, G., Sjogaard, S.S., Petersen, C.M., Nykjaer, A. & Gliemann, J. Tumour necrosis factor
282 alpha-converting enzyme mediates ectodomain shedding of Vps10p-domain receptor family
283 members. *Biochem J* **395**, 285-293 (2006).
284 21. Ayala, J.E.*, et al.* Standard operating procedures for describing and performing metabolic tests
285 of glucose homeostasis in mice. *Dis Model Mech* **3**, 525-534 (2010).
286 22. Graae, A.S.*, et al.* ADAMTS9 Regulates Skeletal Muscle Insulin Sensitivity Through
287 Extracellular Matrix Alterations. *Diabetes* **68**, 502-514 (2019).
288 23. Hwang, J.B. & Frost, S.C. Effect of alternative glycosylation on insulin receptor processing. *J*
289 *Biol Chem* **274**, 22813-22820 (1999).
290 24. Hermey, G.*, et al.* Characterization of sorCS1, an alternatively spliced receptor with completely
291 different cytoplasmic domains that mediate different trafficking in cells. *J Biol Chem* **278**, 7390-
292 7396 (2003).
293 25. Januliene, D.*, et al.* Hidden Twins: SorCS Neuroreceptors Form Stable Dimers. *J Mol Biol* **429**,
294 2907-2917 (2017).
295 26. Kerppola, T.K. Design and implementation of bimolecular fluorescence complementation (BiFC)
296 assays for the visualization of protein interactions in living cells. *Nat Protoc* **1**, 1278-1286 (2006).
297

Figure 1

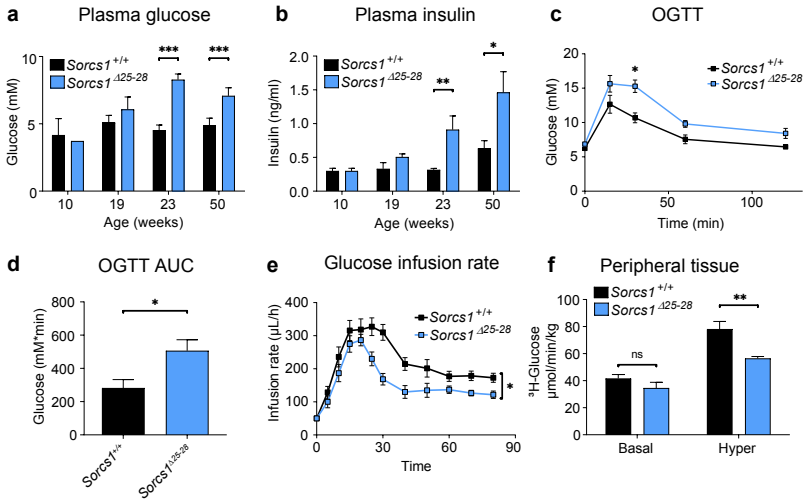
a
Plasma glucose
Sorcs1 +/+
Sorcs1 Δ25-28
Glucose (mM)
Age (weeks)
b
Plasma insulin
Insulin (ng/ml)
Age (weeks)
c
OGTT
Glucose (mM)
Time (min)
d
OGTT AUC
Glucose (mM*min)
e
Glucose infusion rate
Infusion rate (µL/h)
Time
f
Peripheral tissue
³H-Glucose µmol/min/kg
ns
Basal
Hyper

Figure 2

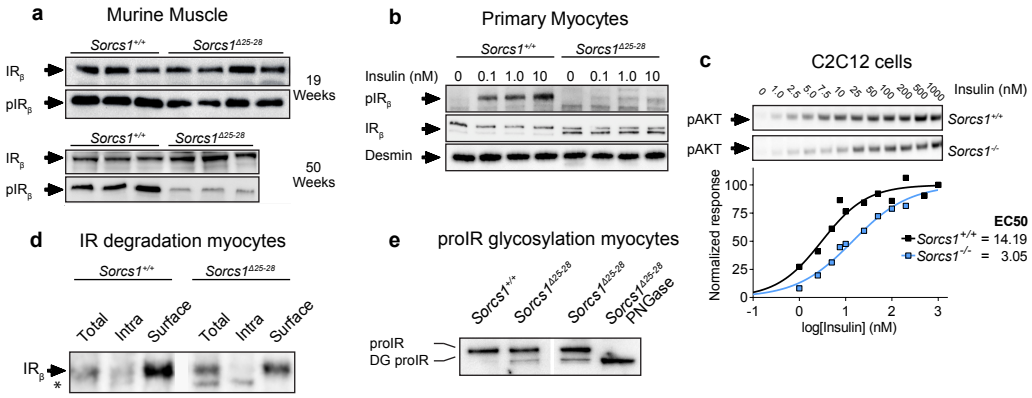
a
Murine Muscle
Sorcs1+/+
Sorcs1Δ25-28
IRβ
pIRβ
19 Weeks
50 Weeks
b
Primary Myocytes
Insulin (nM)
0 0.1 1.0 10 0 0.1 1.0 10
Desmin
c
C2C12 cells
0 1.0 2.5 5.0 7.5 10 25 50 100 200 500 1000
Insulin (nM)
pAKT
Sorcs1-/-
Normalized response
log[Insulin] (nM)
EC50
Sorcs1+/+ = 14.19
Sorcs1-/- = 3.05
d
IR degradation myocytes
Total
Intra
Surface
e
proIR glycosylation myocytes
PNGase
proIR
DG proIR

Figure 3

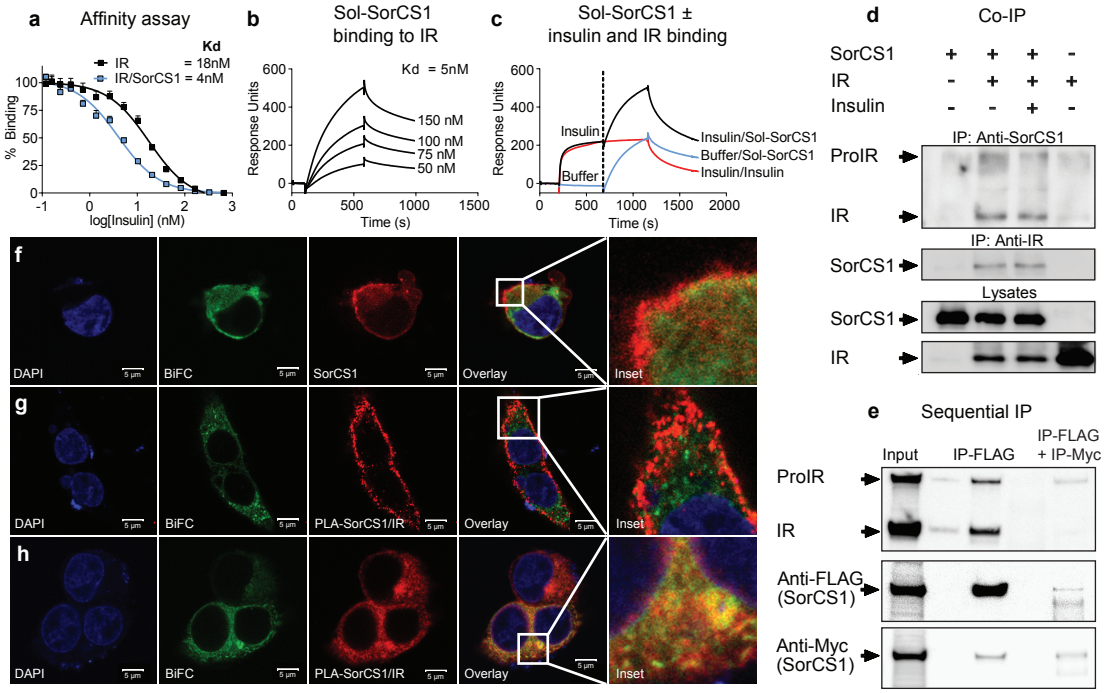
a
Affinity assay
Kd
IR = 18nM
IR/SorCS1 = 4nM
% Binding
log[Insulin] (nM)
b
Sol-SorCS1 binding to IR
Kd = 5nM
150 nM
100 nM
75 nM
50 nM
Response Units
Time (s)
c
Sol-SorCS1 ± insulin and IR binding
Insulin
Buffer
Insulin/Sol-SorCS1
Buffer/Sol-SorCS1
Insulin/Insulin
Response Units
Time (s)
d
Co-IP
SorCS1
IR
Insulin
IP: Anti-SorCS1
ProIR
IR
IP: Anti-IR
SorCS1
Lysates
SorCS1
IR
e
Sequential IP
Input
IP-FLAG
IP-FLAG + IP-Myc
ProIR
IR
Anti-FLAG (SorCS1)
Anti-Myc (SorCS1)
f
DAPI
BiFC
SorCS1
Overlay
Inset
g
DAPI
BiFC
PLA-SorCS1/IR
Overlay
Inset
h
DAPI
BiFC
PLA-SorCS1/IR
Overlay
Inset

Figure 4

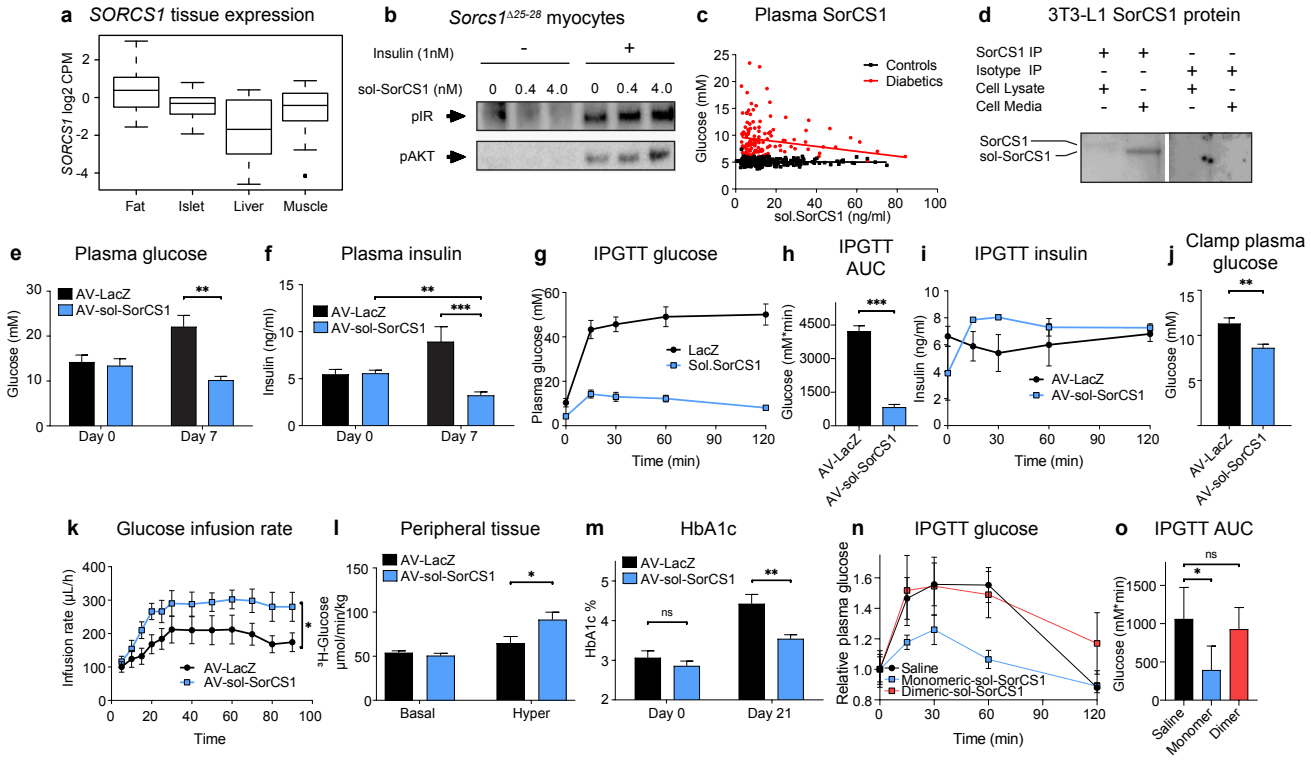
a SORCS1 tissue expression
SORCS1 log2 CPM
Fat
Islet
Liver
Muscle
b Sorcs1Δ25-28 myocytes
Insulin (1nM)
sol-SorCS1 (nM)
0 0.4 4.0 0 0.4 4.0
pIR
pAKT
c Plasma SorCS1
Controls
Diabetics
Glucose (mM)
sol.SorCS1 (ng/ml)
d 3T3-L1 SorCS1 protein
SorCS1 IP
Isotype IP
Cell Lysate
Cell Media
SorCS1
sol-SorCS1
e Plasma glucose
AV-LacZ
AV-sol-SorCS1
Glucose (mM)
Day 0
Day 7
f Plasma insulin
Insulin (ng/ml)
g IPGTT glucose
Plasma glucose (mM)
LacZ
Sol.SorCS1
Time (min)
h IPGTT AUC
Glucose (mM*min)
i IPGTT insulin
Insulin (ng/ml)
j Clamp plasma glucose
k Glucose infusion rate
Infusion rate (µL/h)
Time
l Peripheral tissue
3H-Glucose µmol/min/kg
Basal
Hyper
m HbA1c
HbA1c %
ns
Day 0
Day 21
n IPGTT glucose
Relative plasma glucose
Saline
Monomeric-sol-SorCS1
Dimeric-sol-SorCS1
o IPGTT AUC
Glucose (mM*min)
Saline
Monomer
Dimer